

PAPER • OPEN ACCESS

Compressive strength of concrete specimens with inclusions

To cite this article: M Kovac *et al* 2020 *IOP Conf. Ser.: Mater. Sci. Eng.* **867** 012022

View the [article online](#) for updates and enhancements.

You may also like

- [Effect of the number and arrangement of inclusions on the strength of concrete specimens](#)
M Kovac and S Kusnir
- [Size effect of mortar specimens under uniaxial compression](#)
M Kovac
- [Influence of Mg on Inclusions in 21-4N Valve Steel](#)
Dengping Ji, Beibei Liu, Han Sun et al.



ECS
The
Electrochemical
Society
Advancing solid state &
electrochemical science & technology

DISCOVER
how sustainability
intersects with
electrochemistry & solid
state science research

Compressive strength of concrete specimens with inclusions

M Kovac¹, P Sabol¹, S Kusnir¹, D Kusnirova¹ and M Rovnak¹

¹ Technical university of Kosice, Faculty of Civil Engineering, Institute of Structural Engineering, Vysokoskolska 4, 042 00 Kosice, Slovakia

Abstract. Large diameters and grain aggregates and/or reinforcing bars can have a negative impact on the strength of concrete elements. Tests of concrete specimens with inclusions under uniaxial compression should contribute to a better understanding of the process of failure of concrete elements. The identification of the unstable phase of the cracking and quantification of the effect of diameters, positions, distances, number and material of inclusions, as well as the relative size of inclusions and matrix on compression strength could provide information for an explanation of the causes of the size effect in compressed structural elements. The introduction of the article provides a brief overview of the problem of concrete structures subjected to uniaxial compression. Attention is paid to the failure mechanisms in the process of loading the test specimens from initial crack formation to specimen collapse. The second part is devoted to the investigation of the size effect of varying dimensions of the test specimens with one or three inclusions.

1. Introduction

In 1925, Gonnerman was the first to investigate axial-compressed concrete elements. The influences of the sizes of concrete blocks and cylinders on their nominal compressive strength were analysed based on experimental results [1]. Compression failure is a complex process because the number of non-critical cracks is much greater than tensile failure [2]. It was found that there were cracks in the concrete specimen before the mechanical load was applied. One of the main causes of this phenomenon is cracks due to concrete shrinkage [3]. Concrete is a complex heterogeneous system. Wittmann [4] was the first to introduce three different levels of concrete models: macro-level, meso-level and micro-level. Concrete in the meso-level model can be considered as a material consisting of grains of aggregate, cement putty and transition zone. It has been found that the aggregate grain and the cement putty exhibit almost linear elastic brittle behaviour under axial compression. However, the curve of the $\sigma - \varepsilon$ of ordinary concrete has a typical curvature, which is caused by the interface between the aggregate grain and the cement putty, where the first cracks arise under load. As the load increases, cracks penetrate into the matrix. In this way, an interconnected network of cracks forms in the matrix and at the matrix/aggregate grain boundary until the specimen fails [5].

When designing concrete structures, the compressive strength of the concrete, which is determined from the standard dimensions of test specimens tested in the laboratory, is very important. However, these dimensions do not correspond to the proposed dimensions of concrete elements in real constructions. According to experimental research and analytical studies performed so far, it is possible to generalize the principle of dimensional effect in the design of concrete structures. The strength of the specimens decreases with increasing specimen size and thus larger concrete specimens show lower strength and vice versa, smaller specimens show higher strength [2].



2. Concrete failure mechanisms

Depending on the approach of the concrete model at the macro- and meso-level, we distinguish the different failure mechanisms in the concrete with the acting axial compression. Basically, three types of microcracks can be categorized [2]:

- Cracks at the interface of the cement matrix and aggregate.
- Cracks in the material matrix.
- Cracks passing through the aggregate.

2.1. Meso-level concrete model

Cracks in the concrete can develop and spread due to the concentration of tensile and compressive stresses in the specimen, which occur through the interaction between large aggregate grains and the matrix (figure 1a). A weak connection between the aggregate grain and the cement matrix leads to the initiation of a crack at their interface. The soft matrix flows around the stiffer grains, and thus the lateral deformation in the relatively soft matrix must be greater than in the solid grains of the aggregate, which can lead to transverse tensile and cracks at the interface. The shear stress will develop at the top and below the aggregate grain. Spatial compression is created in these cone-shaped regions, causing the matrix to fail in these regions. The failure then proceeds to grow the crack along the side of the cone (figure 1b). E_a indicates Young's modulus of aggregate and E_m Young's modulus of the matrix. The type of failure and the course of crack propagation depend largely on the ratio of stiffness between matrix and inclusion. The inclusions may be represented by aggregate grain, reinforcing bars or cavities and macropores in the matrix. The cleavage of the lightweight aggregate grain results in a lower stiffness value compared to the stiffness of the surrounding matrix (figure 1c). Fragmentation of the matrix occurs in the case of stress concentrations around large air inclusions (figure 1d). It is generally assumed that in the field of compressive stress, the formation and development of cracks are parallel to the direction of the compressive load. However, the real propagation of micro-cracks caused by axial compression does not correspond to the above assumption. Cracks at the interface between the aggregate grain and the matrix often divert to the sides of the matrix (figure 1e) [6]. The local crushing mechanism of concrete occurs in the interface transition zone (ITZ) when pore concentrations occur above and below the aggregate (figure 1f) [7].

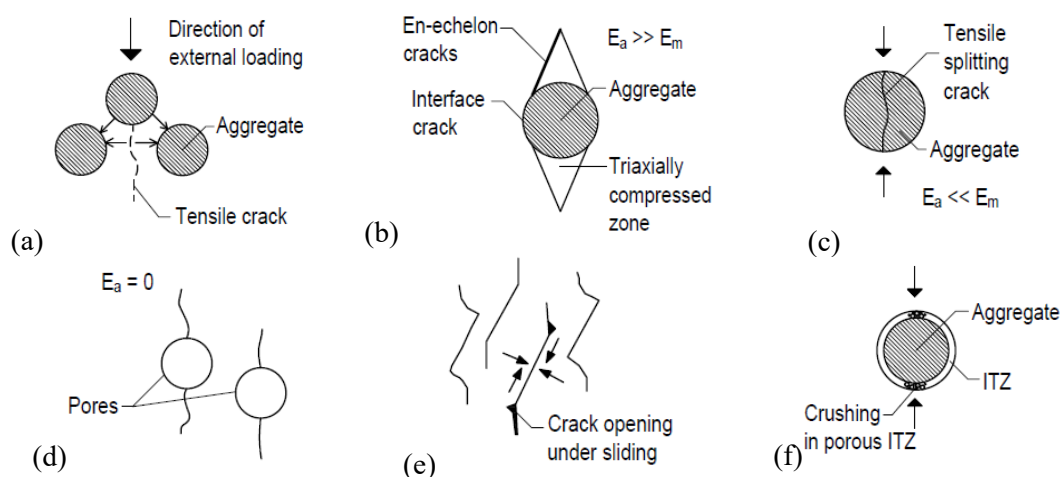


Figure 1. Mechanisms of crack formation and propagation in concrete.

2.2. Macro-level concrete model

The crack propagation process and the failure pattern of the test specimen depend on the design of the experimental equipment, the mode of loading, the boundary conditions and the slenderness (ratio h/d) of the concrete elements. The propagation of macrocracks in the specimen depends on the orientation and magnitude of the shear stress on the contact between the specimen and the load plate. The rigid load plates cause shear stress on the contact which prevents horizontal displacement of the specimen in the

transverse direction and thus creates a region of compressive stress under the plate. If a flexible load plate is used, the lateral displacement is greater than in concrete and the shear stresses are applied outwards from the centre of the specimen. The result is the tensile stress in the matrix. If the stress exceeds the concrete tensile strength, there is a split - tensile cracks in the transverse direction. The mentioned types of boundary conditions in combination with the specimen size ratio (slenderness = height/diameter) h/d determine the mode of failure of the test specimen. In the case of greater slenderness of concrete elements with a ratio $h/d > 2$ and using a rigid steel plate, the specimen may be cutted off due to a slanted crack. On the other hand, the use of an elastic plate causes a transverse tension, i.e. splitting. At the ratio $h/d \leq 1$ and the resilient plate, cleavage also occurs, but with a higher density of cracks in the specimen. At a smaller h/d ratio and a rigid plate, the crushing of the concrete body prevails (figure 2a and figure 2b) [6].

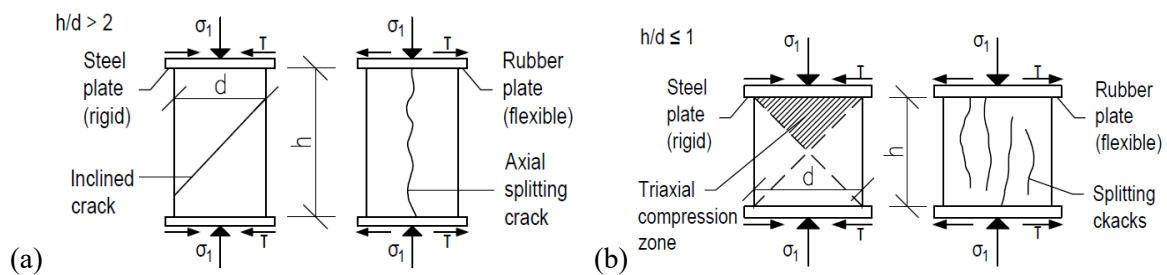


Figure 2. Different mechanisms of concrete failure under uniaxial compression.

3. Experimental research

3.1. Material and specimens

The compression tests were performed on specimens of three different sizes (100×100×50; 150×150×50 and 200×200×50 mm), with 1 or 3 inclusions and two different types of inclusion/matrix interface: steel inclusion/concrete matrix (*S*) and steel inclusion/epoxy/concrete matrix (*SI*). To prepare the specimens, dry concrete mix class C16/20 was used. The test specimens were cast into the steel framework where the inclusions were previously glued in the desired position. At the same time, the prisms were concreted to determine the material characteristics of the concrete. The specimens were tested 7 days after the concreting. During the storage, relative humidity and temperature of the environment were measured every 15 minutes. The diameter of the inclusions was 20, 30 and 40 mm. Their height was identical to the depth of the specimens 50 mm. Figure 3 shows uncoated steel rollers, which were used as the steel inclusion in the specimen, intended to test the inclusion-concrete matrix interface (*S*). Figure 4 shows steel rollers with an epoxy layer with an approximate thickness of 1 mm, which were used as the steel inclusion in the specimen intended to test the inclusion-epoxy-concrete matrix interface (*SI*).



Figure 3. Steel inclusions ($\phi = 20, 30, 40$ mm).



Figure 4. Steel inclusions with epoxide layer ($\phi = 20, 30, 40$ mm).

The inclusions strength class was S235. For the coating of the steel roller, epoxy Sikadur 30 was used. The producer declares the tensile strength of 26 MPa, the compressive strength of 75 MPa, the tensile modulus of 11.2 GPa, and the compressive strength of 9.6 GPa. The strength characteristics of the concrete were measured on the test day. Mean values of concrete compressive strength, modulus of elasticity, flexural strength and splitting tensile strength are given in table 1.

Table 1. Material characteristics of concrete

Inclusion	Specimen	f_{cm} (MPa)	E_{cm} (GPa)	$f_{cf,m}$ (MPa)	$f_{ct,sp,m}$ (MPa)
Steel	SQ-7-100-20-S-2	18.79	18.57	4.01	3.13
	SQ-7-100-20-S-9	19.49	20.32	4.04	3.3
	SQ-7-150-30-S-2	18.57	16.5	4.3	3.03
	SQ-7-150-30-S-9	18.47	19.17	4.2	3.05
	SQ-7-200-40-S-2	19.3	19.7	4.6	2.5
	SQ-7-200-40-S-9	18.5	18.1	4.5	2.4
Steel with epoxide layer	SQ-7-100-20-SI-2	19.51	17.52	3.2	2.27
	SQ-7-100-20-SI-9	14.44	14.59	3.19	2.07
	SQ-7-150-30-SI-2	20.22	19.73	4.5	3.16
	SQ-7-150-30-SI-9	19.9	18.86	4.05	3.18
	SQ-7-200-40-SI-2	15.8	15.2	3.6	2.5
	SQ-7-200-40-SI-9	20.5	17.6	4.4	3.3

3.2. Test arrangement and procedure

Tests were performed by using a loading device consisting of rigid steel plates, threaded rods and a hydraulic jack (figure 5). Test specimens were subjected to uniaxial compression. The tests were controlled by force, the load step was about 9.3 kN. During the test, the vertical deformation of the samples was measured using two indicator gauges. Before the test, the surface of specimens was coated with a white colour and then, the chaotically arranged black dots were applied for non-contact measurement of deformation by photogrammetry GOM Aramis system. Figure 6 (a) shows the specimen before the test and figure 6 (b) shows the typical failure of the specimen after the test.



Figure 5. Arrangement of the uniaxial compression test.

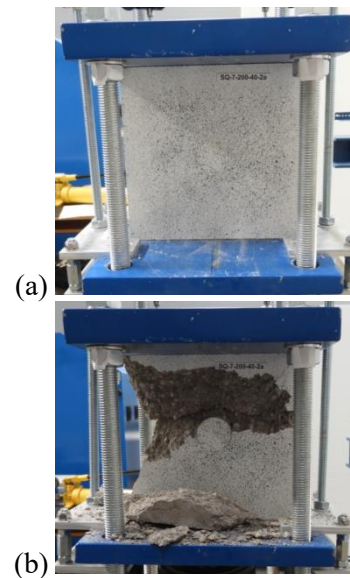


Figure 6. Specimen (a) before (b) after the test.

3.3. Results and discussion

Figure 7 shows the $\sigma/f_{cm} - \epsilon$ relationship of the test specimens with one inclusion in the middle. Test curves with 3 inclusions are shown in figure 8. In the early stages of loading, an elastic phase was identified that changed into the plastic phase and later to overall specimen failure. Rigid steel plates and a load-controlled test caused, that the curves did not show a dominant peak and the post-peak branch. It was found that smaller test specimens showed higher strength and larger specimens achieved less

concrete compressive strength. This tendency can be observed for both single-inclusion and 3-inclusion specimens. In the second case, the impact of significant size effect occurred. The compressive stress at the failure of specimens decreased as the number of inclusions increased from one to three. This phenomenon was evident in specimens of $200 \times 200 \times 50$ mm and $150 \times 150 \times 50$ mm. The test specimens with dimensions of $100 \times 100 \times 50$ mm achieved approximately the same strength values. It could be caused by a triaxial compression zone, which represents a large part of the total sample volume. The comparison of the different inclusion and matrix interface depending on the specimen size revealed changes in the achieved strength values of concrete specimens. Test specimens with 1 and 3 inclusions of $200 \times 200 \times 50$ mm and $150 \times 150 \times 50$ mm with the *SI*-interface exhibited higher strengths than *S*-interface.

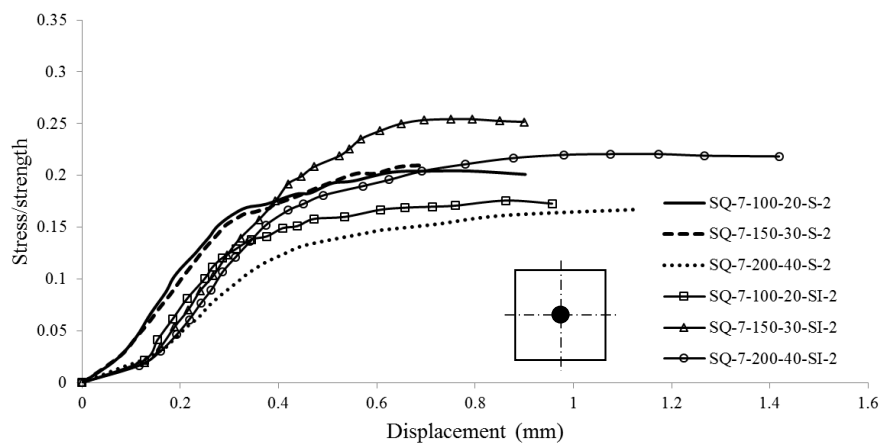


Figure 7. Stress-concrete strength ratio vs displacement of specimens with steel inclusions and steel inclusions with epoxide layer.

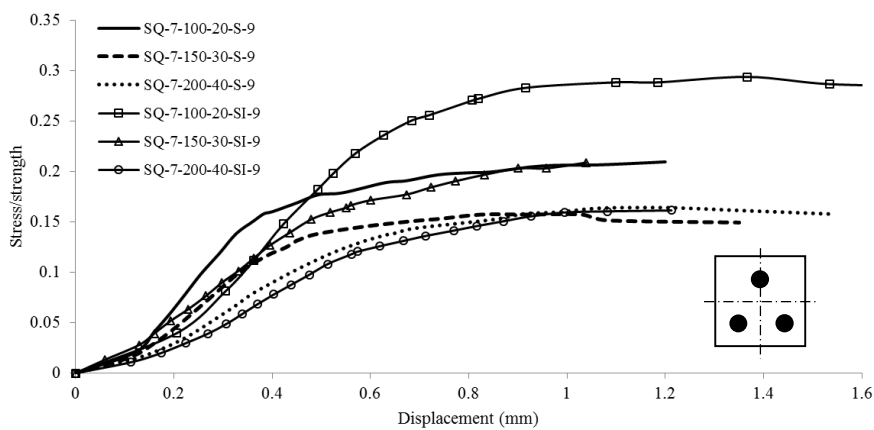


Figure 8. Stress-concrete strength ratio vs displacement of specimens with three steel inclusions and steel inclusions with epoxide layer.

Figure 9 shows the failure of specimens of three different dimensions with 1 inclusion and *S*-interface, and figure 10 shows the failure of test specimens with 1 inclusion and *SI*-interface.

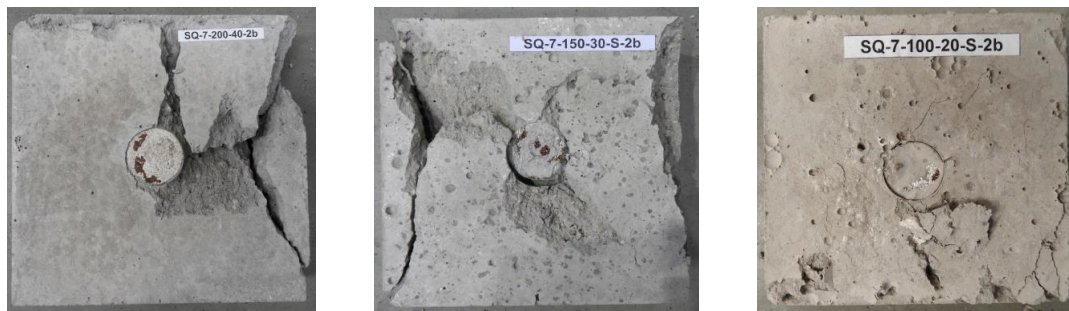


Figure 9. Failure of specimens with *S*-interface (Images size ratio 1:0.75:0.5).



Figure 10. Failure of specimens with *SI*-interface (Images size ratio 1:0.75:0.5).

The failure was related to the development and opening of cracks in the vertical direction. Larger test specimens showed a more fragile failure while the smallest test specimens showed ductile behaviour. The crack development detected by the Aramis system before the collapse of the 3-inclusion test specimens and the *S*-interface is shown in figure 11 and for the *SI*-interface in figure 12. Based on the performed tests is possible to identify the initiation of cracks at the interface of inclusion and concrete matrix. As the load increased, the cracks subsequently spread into the matrix.

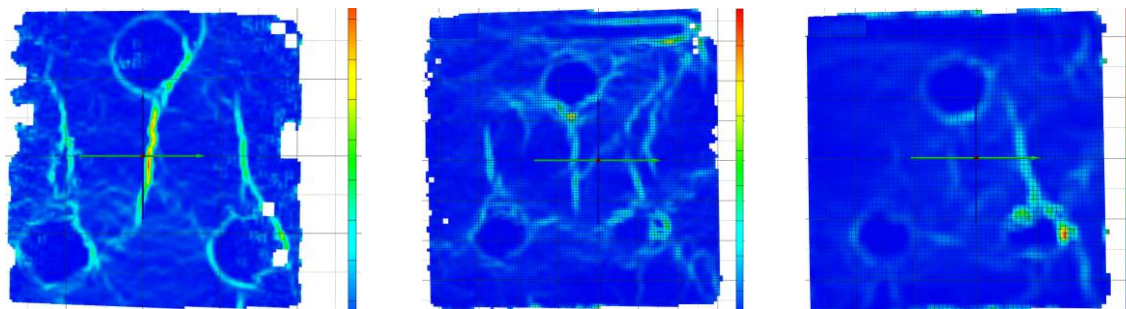


Figure 11. Crack development with *S*-interface (Images size ratio 1:0.75:0.5).

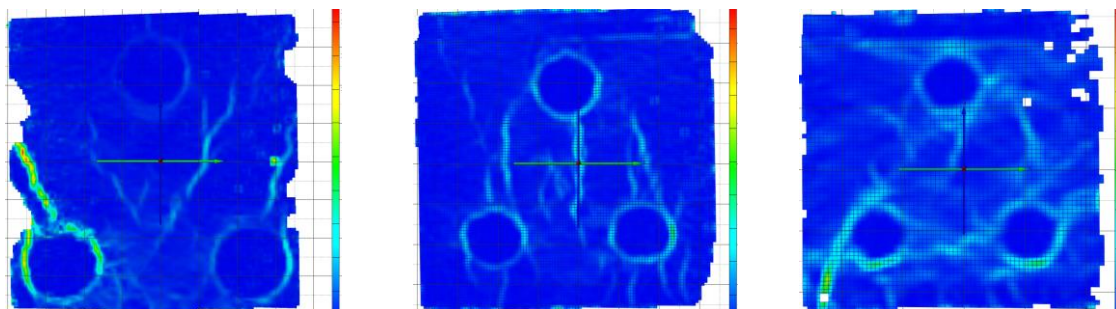


Figure 12. Crack development with *SI*-interface (Images size ratio 1:0.75:0.5).

4. Conclusion

The tests performed and comparison of the test results led to the conclusion that the inclusions contained in the specimens significantly affected their strength to uniaxial compression. The strength of specimens with inclusions was not only affected by the number of inclusions but they largely depended on the properties of the inclusions, their number and arrangement in the specimen. This experiment confirmed the phenomenon of the size effect - the compressive strength of specimens decreased with the increasing size of the specimen. The decrease in the strength of specimens was found with an increasing number of inclusions placed in the specimens.

Based on an overview of the factors and results of tests performed, it can be concluded that further investigation of the mechanisms of failure of the concrete elements stressed by axial compression is necessary for the formation of cracks at the interface and their spread into the matrix depending on stiffness, size, number and arrangement of inclusions. It is necessary to define the relationship between the strength of concrete test specimens and the number and arrangement of inclusion with different material interfaces. It is also useful to look at ways of formation and propagation of cracks during loading, which in turn affects the failure mode of the specimens and have a major impact on the value of strength.

5. References

- [1] Gonnerman H F 1925 Effect of Size and Shape of Test Specimen on Compressive Strength of Concrete *Proc. Am. Soc. Testing Malts* vol 25 part II pp 237-250
- [2] Van Mier J G M 1984 *Strain-softening of concrete under multiaxial loading conditions* PhD Thesis (Netherlands: Eindhoven University of Technology)
- [3] Hsu T T C and Slate F O 1963 Tensile bond strength between aggregate and cement paste or mortar *Journal of the American Concrete Institute Proc.* **60** 465-86
- [4] Wittmann F H 1983 Structure of Concrete with respect to Crack Formation *Fracture Mechanics of Concrete*, ed F H Wittmann (Amsterdam: Elsevier Science Publishers) pp 43-74
- [5] Neville A M 1997 Aggregate bond and modulus of elasticity of concrete *ACI Materials Journal.* **94** 71-74
- [6] Van Mier J G M 1998 Failure of concrete under uniaxial compression: An overview *3rd Int. Conf. on Fracture Mechanics of Concrete and Concrete Structures: Proc. FraMCoS* (Gifu, Japan) ed H Mihashi and K Rokugo (Freiburg: AEDIFICATIO) pp 1169-1182
- [7] Bongers H 1998 Multilevel analysis of concrete in multiaxial compression *Computational Modelling of Concrete Structures*, ed R de Borst et al pp 347-354

Acknowledgments

This work was supported by the Slovak Research and Development Agency under the contract No. APVV-15-0777.